Molecular Crystals and Liquid Crystals Incorporating Nonlinear Optics
Publication details, including instructions for authors and subscription information:
http://www.tandfonline.com/loi/gmcl17

Symmetry-Controlled Electron Correlation Mechanism for Third Order Nonlinear Optical Properties of Conjugated Linear Chains

J. R. Heflin [a], K. Y. Wong [a], O. Zamani-khamiri [a] & A. F. Garito [a]
[a] Department of Physics and Laboratory for Research on the Structure of Matter, University of Pennsylvania, Philadelphia, PA, 19104
Version of record first published: 28 Mar 2007.

To cite this article: J. R. Heflin , K. Y. Wong , O. Zamani-khamiri & A. F. Garito (1988): Symmetry-Controlled Electron Correlation Mechanism for Third Order Nonlinear Optical Properties of Conjugated Linear Chains, Molecular Crystals and Liquid Crystals Incorporating Nonlinear Optics, 160:1, 37-51

To link to this article: http://dx.doi.org/10.1080/15421408808082999

Mol. Cryst. Liq. Cryst., 1988, Vol. 160, pp. 37–51
Reprints available directly from the publisher
Photocopying permitted by license only

Printed in the United States of America

Symmetry-Controlled Electron Correlation Mechanism for Third Order Nonlinear Optical Properties of Conjugated Linear Chains†

J. R. HEFLIN, K. Y. WONG, O. ZAMANI-KHAMIRI, and A. F. GARITO

Department of Physics and Laboratory for Research on the Structure of Matter, University of Pennsylvania, Philadelphia, PA 19104

A microscopic many-electron description is reported for the third order dc-induced second harmonic susceptibility $\gamma_{ijkl}(-2\omega;\omega,\omega,0)$ of all *trans*-polyenes. Based on results obtained by self consistent field configuration interaction theory that suitably accounts for electron–electron interactions and by direct comparison with experimental gas phase results, we show that symmetry-controlled electron correlation effects determine the properties and behavior of $\gamma_{ijkl}(-2\omega;\omega,\omega,0)$ for polyene chains of length 4 through 16 carbon sites. Under well-defined symmetry conditions, the many-electron mechanism involves third order virtual excitations to high-lying, strongly electron correlated two-photon ^1A_g states. The major component $\gamma_{xxxx}(-2\omega;\omega,\omega,0)$ with all fields aligned along the chain axis exhibits a power law dependence of 5.4 due to three major factors which are described.

I. INTRODUCTION

Conjugated organic and polymer structures possess unusually large molecular second order $\beta_{ijk}(-\omega_3;\omega_1,\omega_2)$ and third order $\gamma_{ijkl}(-\omega_4;\omega_1,\omega_2,\omega_3)$ nonlinear optical susceptibilities.[1] Microscopic descriptions of the properties and behavior of β_{ijk} and γ_{ijkl} are a principal focus of current nonlinear optics studies, especially the characteristic features of their associated virtual π-electron excitations. While considerable progress has been achieved in understanding second order properties based on many-electron theory, an important case still lacking suitable description is the frequency dependent third order response of conjugated linear chains such as polyenes and polyenynes.[2–8] A major purpose of this

†Presented in part at the XV International Quantum Electronics Conference, Baltimore, April 1987.

report is to present results from an equivalent many-electron description for γ_{ijkl} of finite conjugated chains.

In the case of second order properties of conjugated structures, a series of experimental and theoretical studies[1,8-12] of the frequency dependent β_{ijk} has shown a basic mechanism of correlated motion among π-electrons due to electron–electron interactions that markedly determines the second order virtual processes and β_{ijk}. The frequency dependent second harmonic susceptibility $\beta_{ijk}(-2\omega;\omega,\omega)$ was studied for three principal noncentrosymmetric structures (i) resonant ring structures such as PNA (*p*-nitroaniline) and MNA (2-methyl-4-nitroaniline); (ii) conjugated linear chains such as NMDVDA [*trans-trans* 1-(4-methylphenyl)-8-(4′-nitrophenyl)-1,7-diene-3,5-octadiyne]; and (iii) conjugated cyclic polyenes and quinoid structures such as DCNQI [2-(4-dicyanomethylene cyclohexa-2,5-dienylidine)-imidazolidine], MPC [N-methyl[4 (1H)-pyridinylidene ethylidene]-2,5-cyclohexadien-1-one], and a predicted structure DPHQ [2-(4′-dicyanomethylene *bis* cyclohexa-2,4,5,2′,5′-pentaenylidine)-imidazolidine].

In these studies, the microscopic description of second order properties was obtained from a many-electron theoretical procedure for calculating and analyzing each frequency dependent term of $\beta_{ijk}(-2\omega;\omega,\omega)$. The procedure is a direct summation method based on self consistent field configuration interaction theory (SCF-MO-SDCI) for many-electron systems that includes singly (SCI) and doubly (DCI) excited configurations which take account of electron–electron interactions and describe electron correlations. In each of the three cases, the calculated results for the magnitude, sign, and dispersion of $\beta_{ijk}(-2\omega;\omega,\omega)$ quantitatively agree with experimental results obtained by dc-induced second harmonic generation (DCSHG) dispersion measurements. Important major features of the microscopic description for the second order processes are graphically contained in density matrix contour diagrams. Each diagram represents an individual second order virtual excitation process and illustrates the basic symmetry-controlled mechanism of highly correlated charge separation responsible for the properties and behavior of β_{ijk} of conjugated structures. Such a mechanism is beyond one-electron models since they entirely neglect correlations.

In separate related developments, experimental and theoretical studies of one-photon and two-photon resonant processes in finite chain polyenes and polyenynes of various lengths of N carbon atom sites have demonstrated that the π-electron states are also dominated by electron correlations and that, correspondingly, independent-particle

models are inadequate in these cases as well. One principal feature observed in polyenes, for example, is that below the first optically allowed dominant singlet 1^1B_u state is located a two photon singlet 2^1A_g state.[13,14] Calculations based on PPP and Hubbard models[14-18] have obtained the correct state ordering and have shown that the 2^1A_g state is an electron correlated state that is properly described in the theoretical results only upon inclusion of at least doubly excited configurations (DCI).

In this paper, we discuss a microscopic many-electron description of third order virtual excitations and $\gamma_{ijkl}(-\omega_4;\omega_1,\omega_2,\omega_3)$ of finite chain polyenes of varying lengths from N equal to 4 through 16 carbon atom sites. Elsewhere, we reported[19] recent results for the third harmonic susceptibility $\gamma_{ijkl}(-3\omega;\omega,\omega,\omega)$ of these systems. The present discussion focuses on the origin of the magnitude, sign and dispersion of the DCSHG susceptibility $\gamma_{ijkl}(-2\omega;\omega,\omega,0)$. The third order properties of *trans*-butadiene (BD) ($N = 4$) and *trans*-hexatriene (HT) ($N = 6$) have been experimentally studied in the gas phase both for the magnitude and sign of $\gamma_{ijkl}(-2\omega;\omega,\omega,0)$,[4] thus allowing direct comparison between theoretical and experimental results. Using HT as a specific illustration, we show that symmetry-controlled correlation effects determine the properties and behavior of $\gamma_{ijkl}(-2\omega;\omega,\omega,0)$ and that this correlation mechanism for $\gamma_{ijkl}(-2\omega;\omega,\omega,0)$ is general to the polyene class. The discussion is based on calculated results obtained by the direct summation method for $\gamma_{ijkl}(-2\omega;\omega,\omega,0)$ whose terms are evaluated by SCF-MO-SDCI procedures.

II. THEORETICAL METHOD

Since *trans*-polyenes are centrosymmetric, their second order nonlinear optical susceptibilities $\beta_{ijk}(-\omega_3;\omega_1,\omega_2)$ are zero by symmetry. Thus, DCSHG experiments directly measure the third order susceptibility tensor $\gamma_{ijkl}(-2\omega;\omega,\omega,0)$ which is defined through the expression

$$p_i^{2\omega} = \gamma_{ijkl}(-2\omega;\omega,\omega,0)E_j^{\omega}E_k^{\omega}E_l^0 \tag{1}$$

where $p_i^{2\omega}$ is a component of the molecular polarization induced at a frequency of 2ω in response to an optical field E^{ω} at frequency ω and a dc field E^0. The susceptibility is purely electronic in origin since the fundamental frequency ω and created harmonic at 2ω are well above molecular vibrational and rotational modes but below elec-

tronic resonances. Theoretically, the susceptibility $\gamma_{ijkl}(-2\omega;\omega,\omega,0)$ is obtained from time dependent perturbation theory. The secular divergences due to the zero frequency input are avoided by employing the Bogoliubov-Mitropolsky method of averages,[20,21] which, for centrosymmetric structures, reduces to an expression for $\gamma_{ijkl}(-2\omega;\omega,\omega,0)$ of the following analytic form

$$\gamma_{ijkl}(-2\omega;\omega,\omega,0) = \frac{e^4}{2\hbar^3} \sum_{n_1 n_2 n_3} \left\{ \frac{r^i_{gn_3} r^l_{n_3 n_2} r^j_{n_2 n_1} r^k_{n_1 g}}{(\omega_{n_3 g} - 2\omega)(\omega_{n_2 g} - 2\omega)(\omega_{n_1 g} - \omega)} + \frac{r^j_{gn_3} r^l_{n_3 n_2} r^k_{n_2 n_1} r^i_{n_1 g}}{(\omega_{n_3 g} + \omega)(\omega_{n_2 g} + \omega)(\omega_{n_1 g} + 2\omega)} + \cdots \right\} \tag{2}$$

where the above expression involves a summation of twelve terms altogether. Here $r^i_{n_1 n_2}$ is the matrix element $\langle n_1|r^i|n_2\rangle$, $\hbar\omega_{n_1 g}$ is the excitation energy of state n_1, and the intermediate states n_1, n_2 and n_3 are summed over all the energy eigenstates of the total Hamiltonian with the ground state excluded from n_1 and n_3. The convention has been chosen that the electric fields are represented as $E^\omega \sin(\omega t - \mathbf{k} \cdot \mathbf{r})$.

The individual terms of Eq. (2) were directly evaluated from the singlet state excitation energies and transition dipole moments obtained by configuration interaction (CI) methods. Included are all singly (SCI) and doubly (DCI) excited π-electron configurations in order to describe properly electron correlations and the resulting correlated ^1A_g excited states. (For example, the number of configurations for HT with $N = 6$ are SCI: 9 and DCI: 45, and the total number of states: 55.) The CI π-electron basis sets were obtained by an all valence electron self consistent field (SCF) molecular orbital (MO) method in the rigid lattice CNDO/S approximation. Although the calculation of the ground state includes all of the valence-shell electrons for each atom in the molecule, we need only consider π-electron orbitals in configuration interaction theory since low-lying excitations have predominantly $\pi \rightarrow \pi^*$ character and it has also been generally established that for conjugated molecular systems the π-electron contribution to $\gamma_{ijkl}(-\omega_4;\omega_1,\omega_2,\omega_3)$ dominates that from σ-electrons.

Both lengths and bond angles for the all-*trans* molecular conformations are experimentally determined values, and consequently, the

bond alternation (carbon–carbon bond lengths of 1.34 and 1.46 Å) is treated directly. The coordinate x axis is chosen along the chain axis, and, of the y and z perpendicular axes, the z axis is set normal to the molecular plane. The hopping interaction between all pairs of sites is included, and the electron–electron repulsion is accounted for via the Ohno potential with the repulsion integral between sites A and B given by

$$\gamma_{AB} = \frac{14.397 \text{ eV}}{\{[(28.794 \text{ Å/eV})/(\gamma_{AA} + \gamma_{BB})]^2 + [R_{AB}(\text{Å})]^2\}^{1/2}} \quad (3)$$

where γ_{AA} and γ_{BB} are empirical intra-atomic repulsion integrals and R_{AB} is the interatomic distance. The calculations were performed on the CRAY X-MP of the Pittsburgh Supercomputing Center.

One measure of the success of the calculation methods is provided by the comparison between calculated and experimental transition energies of the lowest-lying excited states. The optical absorption spectra of polyenes are dominated by the lowest-lying ^1B_u excitation denoted by 1^1B_u. As an example, our calculated values for the 1^1B_u excitation energies of BD and HT, 5.77 and 4.94 eV respectively, are in good agreement with the corresponding experimental vertical excitation energies of 5.91 and 4.93 eV.[14] Comparison is made to vertical rather than 0–0 transitions because the chain geometry is taken as frozen in the calculation. Also of fundamental importance to the study of polyenes is the one-photon forbidden ^1A_g state which has been found to lie below the 1^1B_u. These states are much more difficult to observe, particularly for the shortest chains, and are still the subject of intense experimental spectroscopic effort. The 0–0 transition energy of the 2^1A_g two-photon state of BD has recently been identified[22] at 5.4 eV and compares well to the calculated vertical energy of 5.31 eV. For HT, experimental data[23] is only available for the dimethyl-substituted chain in which the 2^1A_g state is observed at 4.0 ± 0.2 eV as compared to the calculated value of 4.59 eV for HT. Similar satisfactory agreement between experimental and calculated transition energies for the 2^1A_g and 1^1B_u states is also found for the longer polyenes we have studied.

III. DISCUSSION

We will focus discussion on the important example of HT since the gas phase value and sign of $\gamma_{ijkl}(-2\omega;\omega,\omega,0)$ at 1.787 eV (λ = 0.694

TABLE I

The calculated energies and x-components of transition dipole moments with the ground and 1^1B_u states for the lowest-lying states of HT. These transition moments are the ones most significant to $\gamma_{xxxx}(-2\omega;\omega,\omega,0)$ and also illustrate the basic symmetry rules amongst the states.

State	Energy (eV)	$\mu^x_{g,n}$ (D)	$\mu^x_{1^1B_u,n}$ (D)
2^1A_g	4.59	0.0	2.0
1^1B_u	4.94	6.6	0.0
2^1B_u	5.22	0.3	0.0
3^1A_g	6.69	0.0	2.0
4^1A_g	6.80	0.0	1.2
3^1B_u	7.55	0.6	0.0
5^1A_g	7.97	0.0	11.0
4^1B_u	8.07	1.0	0.0

μm) have been carefully determined using gas phase DCSHG. The results for HT thus first serve as comparison between theory and experiment, and afterward, principal results for other length chains are discussed. Because the polyenes are members of the C_{2h} symmetry group, all of the π-electronic states must possess either A_g or B_u symmetry. Since the ground state is always ^1A_g, the ^1B_u excited states are one-photon allowed and two-photon forbidden; and the optical transition to the first ^1B_u excited state is the well-known dominant peak in the linear absorption spectrum. In contrast, the ^1A_g excited states are one-photon forbidden and directly observable optically only by two-photon spectroscopy. The parity selection rules are illustrated by the results for the lowest-lying states of HT in Table I which lists each x-component of the transition dipole moment $\mu^x_{g,n}$ between excited state n and the ground state g, and the x-component of the transition moment $\mu^x_{1^1B_u,n}$ between the excited state n and the 1^1B_u state. Further, it will be shown that $\gamma_{ijkl}(-2\omega;\omega,\omega,0)$ is dominated by virtual transitions among states that have large values for these transition dipole moments.

The calculated values for the independent tensor components of $\gamma_{ijkl}(-2\omega;\omega,\omega,0)$ of HT at a nonresonant fundamental photon energy of 1.787 eV ($\lambda = 0.694$ μm) are $\gamma_{xxxx} = 49.7$, $\gamma_{xyyx} = 4.9$, $\gamma_{yxxy} = 3.5$, $\gamma_{xxyy} = 3.4$, $\gamma_{yyxx} = 2.6$, and $\gamma_{yyyy} = 1.2 \times 10^{-36}$ esu. Components of the form γ_{ijij} are necessarily equal to γ_{iijj} by symmetry of the second and third indices. All components vanish that involve the z-direction perpendicular to the molecular plane because of the antisymmetry of the π orbitals. The results demonstrate clearly that, as

expected, the γ_{xxxx} component with all fields along the direction of conjugation is far larger than the other components.

In gas phase DCSHG experiments, since the molecules are isotropically oriented, the measured value for the third order susceptibility necessarily involves orientational averaging over the different tensor components. The averaged gas phase susceptibility $\gamma_g(-2\omega;\omega,\omega,0)$ is then related to the susceptibility tensor components by the expression

$$\gamma_g = \frac{1}{5}\left[\sum_i \gamma_{iiii} + \frac{1}{3}\sum_{i\neq j}(\gamma_{iijj} + \gamma_{ijij} + \gamma_{ijji})\right] \tag{4}$$

where the indices i and j represent the Cartesian coordinates x, y and z. The experimentally obtained[4] value of γ_g for HT at 1.787 eV is $11.30 \pm 1.05 \times 10^{-36}$ esu[24], and the calculated value for γ_g from Eq. (4) is 11.5×10^{-36} esu. Here we note that the susceptibility thus calculated is solely the π-electron contribution. Although we anticipate the σ-electron contribution to γ_g to be negligible for longer chains, it should have some contribution in the shorter chain cases. After adding the σ-contribution estimated in Ref. 4 of 2.4×10^{-36} esu, we obtain the γ_g value of 13.9×10^{-36} esu, which is still in good correspondence with the experimental result. Experimental measurements were also performed on BD. Our calculated result for γ_g is 2.1×10^{-36} esu at 1.787 eV for the π-contribution to γ_g. After adding in the estimated value 1.5×10^{-36} esu for the σ-contribution, we obtain 3.6×10^{-36} esu for γ_g, which is also in good agreement with the experimental value[4] of $3.45 \pm 0.20 \times 10^{-36}$ esu at 1.787 eV. Importantly, in addition to the magnitudes of γ_g, the calculated results are in agreement with the experimental determination that, at low frequencies, the sign of the nonresonant γ_g is positive in each case.

The third order virtual excitation processes in the polyenes and their contribution to $\gamma_{ijkl}(-2\omega;\omega,\omega,0)$ follow basic symmetry considerations. As evident from Eq. (2), all terms in γ_{ijkl} connect the ground state to itself through three virtual singlet intermediate states via four dipole moment operators. For centrosymmetric conjugated chains, electronic states have definite parity, and the one-photon transition moment vanishes between states of like parity. In a third order process, states must be connected in the series $g \rightarrow {}^1B_u \rightarrow {}^1A_g \rightarrow {}^1B_u \rightarrow g$. Therefore, virtual transitions to both one-photon and two-photon states are necessarily involved. In the summation over intermediate states for HT, for example, there are two major terms which constitute 95% of γ_{xxxx}. In both of these terms, the ${}^1B_u$ state involved is

the dominant low-lying one-photon 1^1B_u π-electron excited state. In addition to its low energy, the importance of this state lies in the value of its transition dipole moment $\mu_{1^1B_u g}^x$ with the ground state of 6.6 D being the largest of all those that involve the ground state.

For one of the significant terms, the intermediate ^1A_g state is the ground state itself, but our finding of another energetically high-lying ^1A_g state is most important. Our calculations indicate that this state is the 5^1A_g state of HT lying at 7.97 eV. Since the 5^1A_g state has a transition moment with 1^1B_u of 11.0 D., it is much more significant than the first two-photon state 2^1A_g which has a corresponding transition moment of only 2.0 D.

The numerators in the γ_{xxxx} component are positive definite because both of these terms have the 1^1B_u as both the first and third intermediate states. Below the first resonance, each of the three factors in the denominator of the first term of Eq. (2) (which is the largest) is also positive when the second intermediate state is the 5^1A_g state. Thus, when the second state is the 5^1A_g state, the contributing term to γ_{xxxx} is positive in sign. However, when the second state is the ground state, the 2ω factor is negative, leading to an overall negative contribution to γ_{xxxx}. The two dominant terms in γ_{xxxx}, therefore, contribute with opposite sign. Since the positive term of the 5^1A_g state is the larger term, the sign calculated for γ_{xxxx} is positive, and, in turn, the measured isotropic average susceptibility γ_g is also positive.

The 1^1B_u, state is 96% comprised of a singly excited configuration of an electron from the highest occupied MO to the lowest unoccupied MO. The 2^1A_g and 5^1A_g states, on the other hand, are nearly 60% comprised of doubly excited configurations. The important distinction for γ_{xxxx} between these two highly electron correlated states is made most evident by the transition density matrix $\rho_{nn'}$, defined through the expression

$$\langle \mu_{nn'} \rangle = -e \int r \, \rho_{nn'}(r) \, dr \tag{5}$$

with

$$\rho_{nn'}(r_1) = \int \psi_n^*(r_1, r_2, \ldots r_M) \psi_{n'}(r_1, r_2, \ldots r_M) dr_2 \ldots dr_M \tag{6}$$

where M is the number of valence electrons included in the molecular wavefunction. Contour diagrams for ρ_{nn}, of the ground, 2^1A_g, and 5^1A_g states with the 1^1B_u state are shown in Figure 1 where solid and

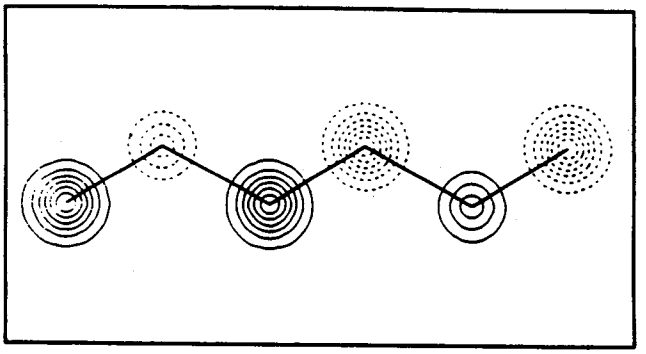

(a)

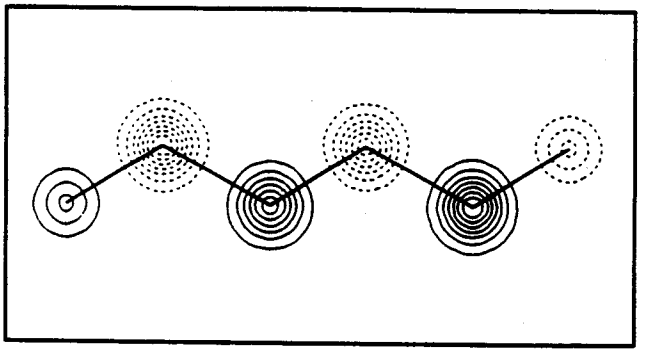

(b)

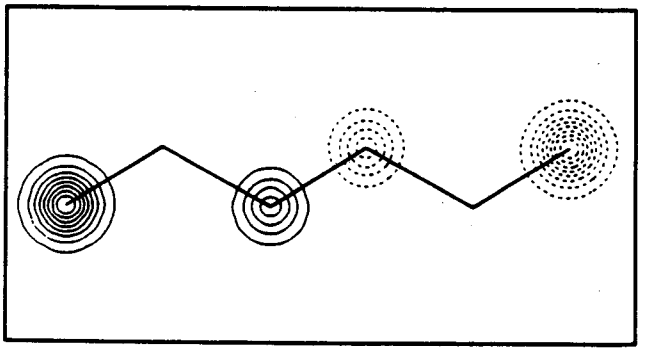

(c)

FIGURE 1 Transition density matrix contour diagrams for the (a) ground, (b) 2^1A_g, and (c) 5^1A_g states with the 1^1B_u state. The corresponding x-components of the transition dipole moments are 6.6, 2.0, and 11.0 D, respectively.

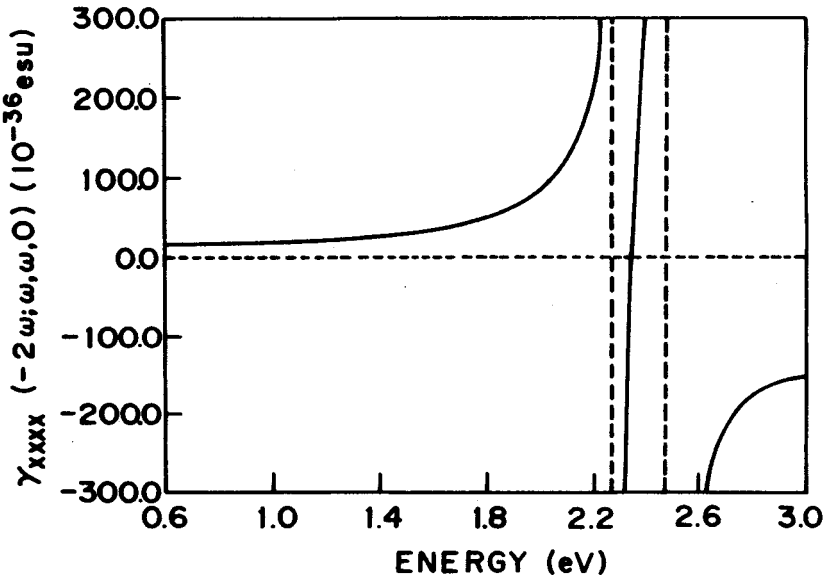

FIGURE 2 Calculated frequency dependence of $\gamma_{xxxx}(-2\omega;\omega,\omega,0)$ for HT. The horizontal axis is the fundamental photon energy. The first vertical dash locates the 2ω resonance to the 2^1A_g state and the second locates the 2ω resonance to the 1^1B_u state.

dashed lines correspond to opposite signs of $\rho_{nn'}$. The contour cut is taken 0.4 Å above the molecular plane since π orbitals vanish on the atoms. The contour diagram of $\rho_{2^1A_g,1^1B_u}$ shows the $2^1A_g \rightarrow 1^1B_u$ transition results in a modulated charge redistribution which yields a small transition moment of 2.0 D, and, correspondingly, a small contribution to γ_{xxxx}. In sharp contrast, $\rho_{5^1A_g,1^1B_u}$ for the virtual transition between the 5^1A_g and 1^1B_u states produces a large charge separation along the chain axis x-direction and an associated large transition moment of 11.0 D which dominates the contributing term to γ_{xxxx}.

Figure 2 displays the calculated dispersion curve for the γ_{xxxx} component of the DCSHG susceptibility of HT from 0.6 eV (λ = 2.07μm) to 3.0 eV (λ = 0.41μm). As can be seen in Eq. (2), there can be 2ω resonances from both ^1B_u and ^1A_g states. The order in which these resonances appear in the DCSHG dispersion is simply the order in which the states occur energetically. Thus, the first singularity in Fig. 2 at 2.30 eV, is the 2ω resonance of the 2^1A_g state, and the singularity at 2.47 eV is the 2ω resonance of the 1^1B_u state. Since these two states are so close in energy, there is rapid variation in γ_{xxxx} in this region. Of course, in real systems natural broadening of the electronic

states will prevent divergence at the resonances and smooth out this variation. In fact, since the 2^1A_g makes such a small conribution below the resonances, when appropriately broadened, it will likely produce only a small peak in the dispersion of γ_{xxxx}.

The general features of the origin of $\gamma_{ijkl}(-2\omega;\omega,\omega,0)$ for HT just described are common to all the chain lengths that we have studied. Importantly, there is a unifying general result that at fixed frequency, $\gamma_{xxxx}(-2\omega;\omega,\omega,0)$ for differing chain lengths exhibits a dramatic but well-defined increase with increased chain length. The values for $\gamma_{xxxx}(-2\omega;\omega,\omega,0)$ at a fundamental photon energy of 0.65 eV (λ = 1.907μm) are plotted against the number of carbon atom sites N on a log–log scale in Figure 3. The good linear fit indicates that γ_{xxxx} possesses a power law dependence upon N with an exponent of 5.4 determined from the slope.

We have identified three length-dependent factors that lead to this rapid growth of $\gamma_{xxxx}(-2\omega;\omega,\omega,0)$. First, the lowest optical excitation energy decreases proportionally to the inverse of the chain length as illustrated, for example, by the lowering from 5.9 eV in butadiene

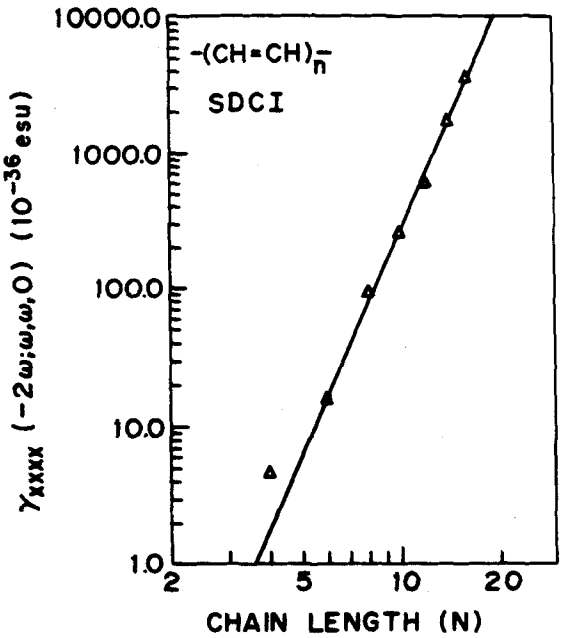

FIGURE 3 Log–log plot of $\gamma_{xxxx}(-2\omega;\omega,\omega,0)$ at 0.65 eV versus the number N of carbon atom sites in the polyene chain at the SDCI level of calculation. Linear fit corresponds to $\gamma_{xxxx} \propto N^{5.4}$.

TABLE II

The x-component of the transition dipole moment between the ground and 1^1B_u states as a function of polyene chain length. The increase in the transition moment with increased chain length demonstrates a general feature found for other transition moments as well.

N (sites)	$\mu^x_{g,1^1B_u}$ (D)
4	5.2
6	6.6
8	7.8
10	8.8
12	9.7
14	11.1
16	12.2

($N = 4$) to 3.7 eV in the case of dodecahexaene ($N = 12$).[14] Although we purposely chose a frequency which is far below the electronic resonances of all the chains we studied, it is clear from Eq. (2) that this factor will contribute to the growth of $\gamma_{xxxx}(-2\omega;\omega,\omega,0)$. Second, the magnitudes of the transition dipole moments along the chain axis increase steadily with chain length. This is illustrated in Table II where the calculated transition dipole moment $\mu^x_{g,1^1B_u}$ between the ground and 1^1B_u states are listed as a function of chain length. Because such virtual excitations naturally produce a charge redistribution over a length comparable to that of the chain, longer chains have larger transition dipole moments and, correspondingly, larger γ_{xxxx} values. Third, although we have pointed out that for HT the nonresonant $\gamma_{xxxx}(-2\omega;\omega,\omega,0)$ is dominated by virtual excitations involving primarily just three π-electron excited states, we have found that for longer chains, an increasingly larger number of both ^1B_u and ^1A_g excited states play a significant role in $\gamma_{xxxx}(-2\omega;\omega,\omega,0)$. Thus, in addition to lower excitation energies and larger transition dipole moments, there is a further increase in $\gamma_{xxxx}(-2\omega;\omega,\omega,0)$ with increased chain length due to larger numbers of significant contributing terms.

The importance of electron correlations to $\gamma_{ijkl}(-2\omega;\omega,\omega,0)$ of the conjugated linear chains is further illustrated by results obtained from calculations at the SCI level that purposely omit doubly-excited configurations (DCI) but are otherwise identical. As illustrated in Fig. 4, at this level of calculation, the values calculated for nonresonant $\gamma_{xxxx}(-2\omega;\omega,\omega,0)$ are negative in sign for all of the polyene chains which is contrary to the experimental results. This disagreement occurs because the SCI calculation improperly describes electron correlation which we have found to be of primary importance, such as

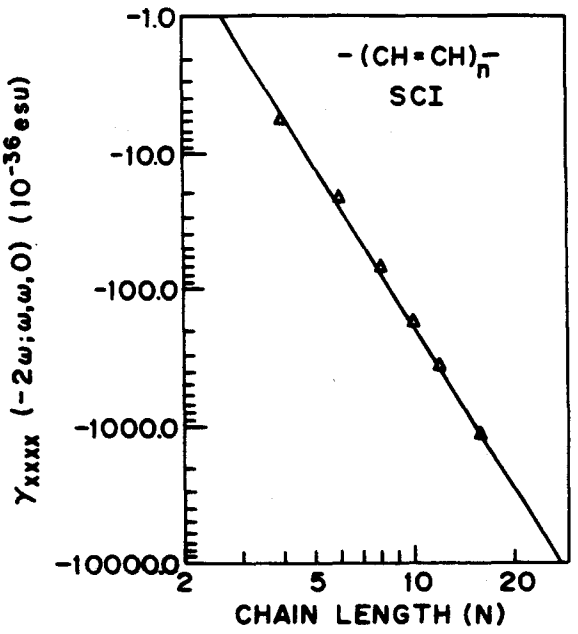

FIGURE 4 Log–log plot of $\gamma_{xxxx}(-2\omega;\omega,\omega,0)$ at 0.65 eV versus the number N of carbon atom sites from a calculation at the SCI level. The calculated values for γ_{xxxx} are negative and the slope corresponds to $\gamma_{xxxx} \propto N^{3.9}$.

in the illustrative case of the 5^1A_g state of HT. Instead, at the SCI level, $\gamma_{xxxx}(-2\omega;\omega,\omega,0)$ is predicted to be dominated solely by the virtual excitation process which involves only the ground and 1^1B_u states. A further consequence of incomplete account of correlation is the prediction of a smaller increase in $\gamma_{xxxx}(-2\omega;\omega,\omega,0)$ with increased chain length. The power law dependence of $\gamma_{xxxx}(-2\omega;\omega,\omega,0)$ on N at the SCI level has an exponent of 3.9 as compared to 5.4 for the full SDCI calculation.

IV. CONCLUSION

In summary, we have shown that symmetry-controlled correlation effects determine the properties and behavior of the third order dc-induced second harmonic susceptibility $\gamma_{ijkl}(-2\omega;\omega,\omega,0)$ of all *trans*-polyenes and that this correlation mechanism is general to the polyene class of differing length chains from $N = 4$ to 16 carbon atoms. Based on the direct summation method for $\gamma_{ijkl}(-2\omega,\omega,\omega,0)$ and self con-

sistent field configuration interaction theory (SCF-MO-SDCI), the calculated magnitudes and signs of $\gamma_{ijkl}(-2\omega;\omega,\omega,0)$ are in good agreement with existing experimental results for two of the shortest chains, namely, butadiene ($N = 4$) and hexatriene ($N = 6$). After showing on general symmetry grounds that two-photon allowed states, as well as one-photon allowed states, must play a role in third order responses, we have identified in detail the significant contributions to $\gamma_{ijkl}(-2\omega;\omega,\omega,0)$ using the case of hexatriene as illustration, and have shown that major terms from high-lying two-photon ^1A_g states determine the magnitude, sign, and dispersion of $\gamma_{ijkl}(-2\omega;\omega,\omega,0)$. We further found that, for the chain lengths $N = 4$ to 16, the major component $\gamma_{xxxx}(-2\omega;\omega,\omega,0)$ exhibits a power law dependence on the chain length with an exponent of 5.4 which results from three length dependent factors. With increased chain length, there are lower excitation energies, larger transition dipole moments, and increased number of contributing excited state terms. Finally, by purposely limited calculations, we further illustrated the necessity of properly accounting for electron correlations in third order virtual excitation processes.

This research was generously supported by AFOSR and DARPA, F49620-85-C-0105 and NSF/MRL, DMR-85-19059.

References

1. See, for example, *Nonlinear Optical Properties of Organic and Polymeric Materials*, edited by D. J. Williams, ACS Symp. Series, Vol. 233 (American Chemical Society, Washington, D. C., 1983) and references therein.
2. A. D. Buckingham, M. P. Bogaard, D. A. Dunmur, C. P. Hobbs and B. J. Orr, *Trans. Faraday Soc.*, **66**, 1548 (1970).
3. J. P. Hermann, D. Ricard and J. Ducuing, *Appl. Phys. Lett.*, **23**, 178 (1973).
4. J. F. Ward and D. S. Elliott, *J. Chem. Phys.*, **69**, 5438 (1978).
5. G. P. Agarwal, C. Cojan and C. Flytzanis, *Phys. Rev.*, **B17**, 776 (1978).
6. E. McIntyre and H. Hameka, *J. Chem. Phys.* **68**, 5534 (1978).
7. D. N. Beratan, J. N. Onuchic and J. W. Perry, *J. Phys. Chem.*, **91**, 2696 (1987).
8. A. F. Garito, C. C. Teng, K. Y. Wong and O. Zamani-Khamiri, *Mol. Cryst. Liq. Cryst.*, **106**, 219 (1984).
9. S. J. Lalama and A. F. Garito, *Phys. Rev.* **A20**, 1179 (1979).
10. C. C. Teng and A. F. Garito, *Phys. Rev. Lett.* **50**, 350 (1983); *Phys. Rev.* **B28**, 6766 (1983).
11. A. F. Garito, Y. M. Cai, H. T. Man and O. Zamani-Khamiri, in *Crystallographically Ordered Polymers*, edited by D. J. Sandman, ACS Symp. Series, Vol. 337 (American Chemical Society, Washington, D. C., 1987) Chap. 14.
12. A. F. Garito, K. Y. Wong and O. Zamani-Khamiri, in *Electroactive Polymers*, edited by D. Ulrich and P. Prasad (Plenum, New York, 1987).
13. B. S. Hudson and B. E. Kohler, *J. Chem. Phys.* **59**, 4984 (1973).
14. See, for example, B. S. Hudson, B. E. Kohler and K. Schulten, in *Excited States*, Vol. 6, edited by E. C. Lim (Academic Press, New York, 1982) p. 1 and reference therein.

15. A. A. Ovchinikov, I. I. Ukrainski and G. V. Kuentsel, *Soviet Phys. Uspekhi*, **15**, 575 (1973) and reference therein.
16. K. Schulten, I. Ohmine and M. Karplus, *J. Chem. Phys.*, **64**, 4422 (1976).
17. I. R. Ducasse, T. E. Miller and Z. G. Soos, *J. Chem. Phys.*, **76**, 4094 (1982).
18. P. Tavan and K. Schulten, *J. Chem. Phys.*, **85**, 6602 (1986); *Phys. Rev.* B**36**, 4337 (1987).
19. J. R. Heflin, K. Y. Wong, O. Zamani-Khamiri and A. F. Garito, Proc. XV Int. Quant. Elec. Conf., p. 114 (1987); *Phys. Rev. B* (submitted).
20. N. N. Bogoliubov and Y. A. Mitropolsky, *Asymptotic Methods in the Theory of Non-Linear Oscillations* (Gordon and Breach, 1961) translated from Russian.
21. B. J. Orr and J. F. Ward, *Molecular Physics*, **20**, 513 (1971).
22. R. R. Chadwick, D. P. Gerrity and B. S. Hudson, *Chem. Phys. Lett.*, **115**, 24 (1985).
23. B. S. Hudson and B. E. Kohler, *Synth. Metals*, **9**, 241 (1984).
24. We have converted Ward and Elliott's $\chi^{(3)}$ to our notation by $\gamma_g(-2\omega;\omega,\omega,0) = 3/2\ \chi^{(3)}$.